ACS OMEGA

Open Access

http://pubs.acs.org/journal/acsodf

Article

Solubility, Thermodynamic Parameters, and Dissolution Properties of 17-α Hydroxyprogesterone in 13 Pure Solvents

Qi Zhao,[⊥] Yinhu Pan,[⊥] Yankai Xiong, Ping Xu, Qianyun Sun, Hemei Yin, and Fumin Xue*

Cite This: *ACS Omega* 2024, 9, 16106−16117

Read Online

ACCESS | Metrics & More | Article Recommendations | Supporting Information

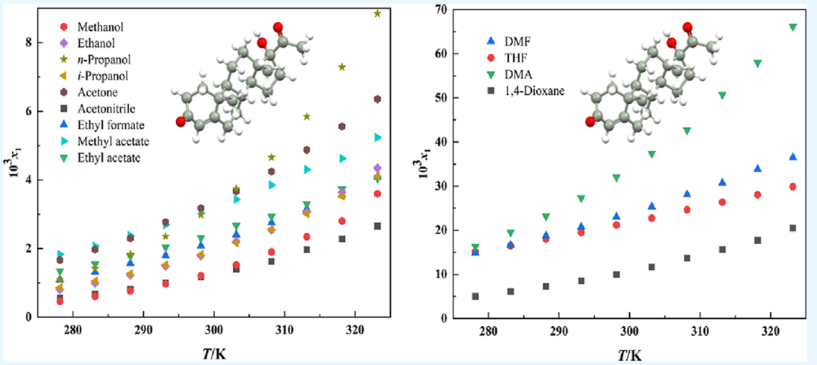

ABSTRACT: The static gravimetric method was used to measure the solubility of 17-α hydroxyprogesterone (OHP) in 13 pure solvents ranging from 278.15 to 323.15 K. The results indicate that the experimental solubility of OHP increases with increasing temperature. The experimental solubility data were correlated by the selected van't Hoff model, λh model, modified Apelblat model, Yaws model, and nonrandom two-liquid (NRTL) model. The fitting results show that the Yaws model can give better correlation results by fitting 13 different pure solvent systems. Based on the NRTL equation, the thermodynamic analysis of solubility data showed that the mixing process was spontaneous. The Hansen solubility parameters (HSPs) and solvent effect were applied to explore these solubility characteristics. Finally, the thermodynamic properties $\Delta_{sol}H^{\circ}$, $\Delta_{sol}S^{\circ}$, $\Delta_{sol}G^{\circ}$, $\%\xi_{H}$, and $\%\xi_{TS}$ were calculated by the van't Hoff model equation. The results showed that $\Delta_{sol}H^{\circ}$, $\Delta_{sol}S^{\circ}$, and $\Delta_{sol}G^{\circ}$ are all positive values, indicating that the dissolution of OHP in the selected solvent is an endothermic reaction with increasing entropy.

1. INTRODUCTION

17-α hydroxyprogesterone[1] (Figure 1, $C_{21}H_{30}O_3$, molar mass: 330.46 g·mol^{-1}, CAS registry no. 68-96-2), with the name

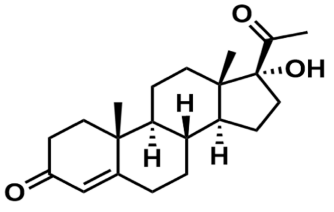

Figure 1. Chemical structure of the OHP.

hydroxyprogesterone, is an endogenous progesterone-like steroid hormone similar to progesterone. It is an important method for diagnosing and screening congenital adrenal hyperplasia in newborns.[2] OHP has been used preventively from the 12th to 37th week of pregnancy, especially in high-risk groups of premature delivery (such as women with a history of premature delivery or spontaneous abortion). In addition, 17-α hydroxyprogesterone (OHP) can also effectively treat neutrophil airway inflammation, including reducing blood and respiratory neutrophils,[3] and controlling the nonincrease in eosinophil[4] count. OHP in serum mainly interacts with sex hormones to promote the development of individual organs.[5] OHP plays a crucial role in pharmacy, medical testing, and other fields.[6,7]

At present, the research on OHP only focuses on the synthesis method and technology, and its crystallization has not been studied. In addition, the literature[8] has been found to elaborate on the role of 17-α hydroxyprogesterone caproate in preventing premature delivery. Generally speaking, solution crystallization is of great significance to the refinement and purification of OHP.[9] On this basis, high-precision solubility data and thermodynamic parameters are obtained, which

Received: December 12, 2023
Revised: March 8, 2024
Accepted: March 13, 2024
Published: March 31, 2024

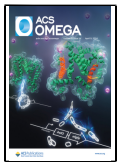

https://doi.org/10.1021/acsomega.3c09922
ACS Omega 2024, 9, 16106−16117

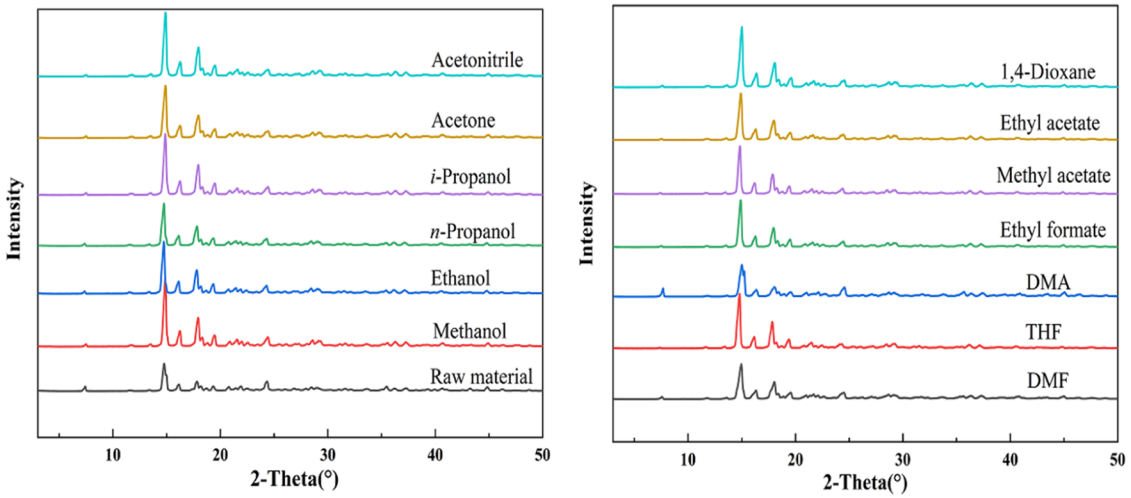

Figure 2. XRPD patterns of the OHP in 13 pure solvents.

provides theoretical basis for the optimal design of crystallization process.[10] However, there is no literature about the solubility and thermodynamic properties of OHP. In detail, the solubility data provide a reference for solvent screening in industrial production. The high solubility of OHP in some solvents provides the possibility to improve production efficiency. In addition, in some solutions, the solubility of the OHP varies with temperature. When separating or purifying the OHP, cooling crystallization or evaporative crystallization can be prioritized. The solubility data provide data support for the preparation of supersaturated solutions. When configuring a supersaturated solution at a specific temperature, the amount of solute and solvent to be added can be calculated based on solubility and supersaturation. Finally, solubility data are also an important basis for calculating the width of the metastable zone. These data provide a basis for the crystal growth of the OHP.

In this work, the solubilities of OHP were measured in 13 pure solvent systems (i.e., methanol, ethanol, *n*-propanol, *i*-propanol, acetone, acetonitrile, *N*,*N*-dimethylformamide (DMF), tetrahydrofuran (THF), *N*,*N*-dimethylacetamide (DMA), ethyl formate, methyl acetate, ethyl acetate, and 1,4-dioxane) from 278.15 to 323.15 K by the static gravimetric method. The van't Hoff model, λh model, modified Apelblat model, Yaws model, and nonrandom two-liquid (NRTL) model were used to correlate the experimental solubility data of OHP in the 13 pure solvent system. The thermodynamic parameters such as Gibbs energy, entropy, and enthalpy were also calculated. The Hansen solubility parameters (HSPs) was used to study the relationship between the solubility order of OHP in different solvents and their miscibility. Furthermore, by analyzing the solvent effect, the influence of solvent on solubility was studied, and the corresponding relationship between solubility and physical and chemical properties of the solvent was established. Finally, we applied the van't Hoff equation to investigate the thermodynamic properties ($\Delta_{sol}H^{\circ}$, $\Delta_{sol}S^{\circ}$, $\Delta_{sol}G^{\circ}$, $\%\xi_H$ and $\%\xi_{TS}$) of the system.

2. RESULTS AND DISCUSSION

2.1. X-ray Powder Diffraction (XRPD) Analysis. In the solubility determination experiment, the solid residues of OHP raw materials and its 13 solvents were determined by X-ray powder diffraction (XRPD). The XRPD data of the measured OHP in this study are shown in Figure 2. The characteristic peaks of OHP in 13 pure solvents are consistent with the raw materials, and the positions of the peaks are almost the same, indicating that the crystal form does not change during the experimental process. Based on the above content, we learn that OHP has not undergone solvation or crystal form transformation in all solvents, let alone amorphous.

2.2. Thermal Analysis. The thermogravimetric analysis (TGA) and differential scanning calorimetry (DSC) curves of the OHP raw materials are shown in Figure 3. It can be seen

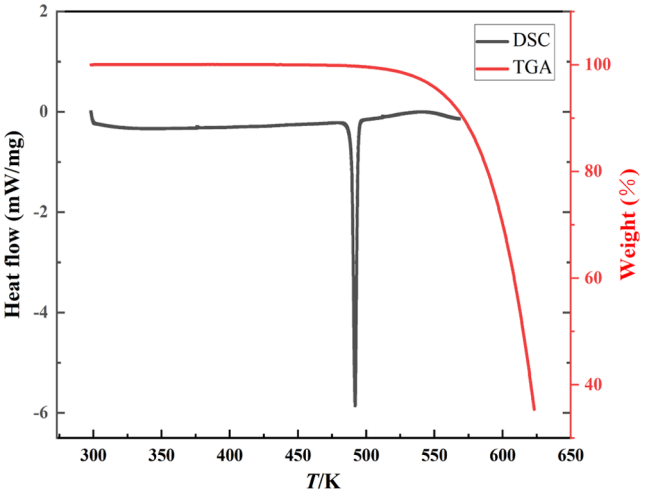

Figure 3. Thermal analysis (TGA and DSC) of the bacterial biomass of the OHP.

from the experimental results that OHP is melted before chemical decomposition. In this study, the melting temperature T_m of the OHP was 490.46 K (standard uncertainty of 0.5 K). No literature has reported its melting point before, so we conducted research on the official Web site data of the manufacturer (≥481.15 K), which is somewhat different from the data we measured. To verify its accuracy, we also searched for some relevant patent reports on the OHP melting point. In patent CN 116143858 A, it was mentioned that the OHP melting point is 492.15−493.15 K, which is not far from what we measured. These subtle differences may be caused by factors such as the purity of OHP, different instruments and

https://doi.org/10.1021/acsomega.3c09922
ACS Omega 2024, 9, 16106−16117

Table 1. Experimental and Fitted Solubility Data of the OHP in 13 Pure Organic Solvents at Temperatures from 278.15 to 323.15 K (P = 0.1 MPa)[a]

T (K)	$10^3x_1^{exp}$	$10^3x_1^{van't\ Hoff}$	$10^3x_1^{\lambda h}$	$10^3x_1^{Apelblat}$	$10^3x_1^{Yaws}$	$10^3x_1^{NRTL}$
			Methanol			
278.15	0.4613	0.4496	0.4512	0.4793	0.4794	0.4700
283.15	0.6032	0.5839	0.5853	0.6071	0.6067	0.5991
288.15	0.7641	0.7514	0.7525	0.7661	0.7654	0.7603
293.15	0.9708	0.9587	0.9593	0.9632	0.9626	0.9604
298.15	1.210	1.213	1.213	1.207	1.207	1.208
303.15	1.524	1.523	1.523	1.508	1.508	1.512
308.15	1.900	1.899	1.898	1.877	1.878	1.885
313.15	2.343	2.350	2.349	2.330	2.331	2.339
318.15	2.798	2.889	2.889	2.883	2.884	2.891
323.15	3.598	3.530	3.531	3.557	3.555	3.557
			Ethanol			
278.15	0.8017	0.7942	0.7990	0.8436	0.8154	0.8218
283.15	0.9918	0.9842	0.9880	1.019	0.9990	0.9975
288.15	1.224	1.211	1.213	1.228	1.218	1.209
293.15	1.485	1.479	1.479	1.479	1.479	1.463
298.15	1.788	1.794	1.793	1.777	1.787	1.767
303.15	2.203	2.162	2.160	2.133	2.150	2.130
308.15	2.539	2.591	2.588	2.556	2.577	2.563
313.15	3.059	3.087	3.084	3.057	3.075	3.076
318.15	3.647	3.657	3.656	3.652	3.655	3.684
323.15	4.343	4.310	4.315	4.355	4.329	4.403
			n-Propanol			
278.15	1.085	1.079	1.080	1.155	1.088	1.098
283.15	1.419	1.410	1.411	1.469	1.417	1.420
288.15	1.831	1.824	1.825	1.863	1.829	1.825
293.15	2.356	2.340	2.340	2.353	2.342	2.330
298.15	2.982	2.977	2.977	2.962	2.975	2.959
303.15	3.741	3.757	3.756	3.717	3.752	3.734
308.15	4.656	4.706	4.705	4.650	4.699	4.686
313.15	5.847	5.852	5.851	5.798	5.846	5.844
318.15	7.285	7.227	7.227	7.209	7.225	7.248
323.15	8.848	8.868	8.869	8.937	8.876	8.945
			i-Propanol			
278.15	0.8587	0.8585	0.8641	0.8586	0.8586	0.8824
283.15	1.047	1.047	1.051	1.047	1.047	1.054
288.15	1.268	1.268	1.270	1.268	1.268	1.258
293.15	1.526	1.526	1.526	1.526	1.526	1.500
298.15	1.824	1.824	1.822	1.824	1.824	1.788
303.15	2.169	2.169	2.165	2.168	2.169	2.129
308.15	2.564	2.564	2.559	2.563	2.564	2.532
313.15	3.014	3.014	3.009	3.014	3.014	3.008
318.15	3.526	3.526	3.525	3.526	3.526	3.567
323.15	4.105	4.105	4.111	4.105	4.105	4.223
			Acetone			
278.15	1.667	1.667	1.681	1.669	1.669	1.724
283.15	1.975	1.976	1.985	1.977	1.977	1.990
288.15	2.300	2.327	2.331	2.327	2.327	2.301
293.15	2.768	2.725	2.724	2.725	2.725	2.667
298.15	3.174	3.174	3.169	3.174	3.174	3.095
303.15	3.667	3.679	3.670	3.678	3.679	3.595
308.15	4.244	4.244	4.233	4.243	4.244	4.180
313.15	4.874	4.874	4.865	4.873	4.873	4.861
318.15	5.557	5.572	5.572	5.573	5.573	5.655
323.15	6.357	6.345	6.360	6.346	6.346	6.578
			Acetonitrile			
278.15	0.5531	0.5524	0.5562	0.5646	0.5542	0.5693
283.15	0.6744	0.6741	0.6768	0.6824	0.6753	0.6792
288.15	0.8123	0.8169	0.8184	0.8209	0.8175	0.8104
293.15	0.9977	0.9835	0.9836	0.9831	0.9834	0.9666

https://doi.org/10.1021/acsomega.3c09922
ACS Omega 2024, 9, 16106−16117

Table 1. continued

T (K)	$10^3 x_1^{exp}$	$10^3 x_1^{van't\ Hoff}$	$10^3 x_1^{\lambda h}$	$10^3 x_1^{Apelblat}$	$10^3 x_1^{Yaws}$	$10^3 x_1^{NRTL}$
298.15	1.177	1.177	1.175	1.172	1.176	1.152
303.15	1.400	1.400	1.397	1.392	1.399	1.373
308.15	1.622	1.655	1.652	1.647	1.654	1.634
313.15	1.973	1.947	1.944	1.940	1.946	1.942
318.15	2.278	2.279	2.278	2.278	2.279	2.306
323.15	2.653	2.655	2.659	2.666	2.656	2.733
			DMF			
278.15	14.87	14.89	15.03	14.81	14.81	15.31
283.15	16.58	16.69	16.77	16.65	16.65	16.80
288.15	18.74	18.64	18.66	18.63	18.64	18.44
293.15	20.73	20.74	20.70	20.76	20.76	20.35
298.15	22.98	22.99	22.91	23.03	23.00	22.49
303.15	25.33	25.40	25.30	25.45	25.45	24.91
308.15	28.09	27.97	27.87	28.02	28.02	27.58
313.15	30.72	30.71	30.64	30.73	30.73	30.64
318.15	33.81	33.61	33.63	33.60	33.60	34.01
323.15	36.47	36.68	36.84	36.61	36.60	37.94
			THF			
278.15	15.18	15.21	15.39	15.11	15.11	15.81
283.15	16.50	16.58	16.67	16.53	16.53	16.71
288.15	18.00	18.02	18.02	18.02	18.02	17.77
293.15	19.47	19.53	19.46	19.56	19.56	19.03
298.15	21.19	21.10	20.99	21.16	21.16	20.45
303.15	22.75	22.75	22.61	22.82	22.82	22.13
308.15	24.62	24.46	24.34	24.52	24.52	23.99
313.15	26.34	26.24	26.18	26.28	26.27	26.15
318.15	28.06	28.09	28.13	28.08	28.08	28.60
323.15	29.87	30.01	30.20	29.92	29.92	31.37
			DMA			
278.15	16.34	16.30	16.26	16.38	16.38	16.13
283.15	19.55	19.47	19.44	19.53	19.53	19.42
288.15	23.20	23.12	23.11	23.14	23.14	23.20
293.15	27.32	27.29	27.29	27.28	27.28	27.52
298.15	32.06	32.03	32.05	32.00	32.00	32.37
303.15	37.41	37.40	37.43	37.35	37.35	37.78
308.15	42.66	43.46	43.49	43.40	43.40	44.07
313.15	50.75	50.25	50.27	50.21	50.21	50.07
318.15	58.00	57.83	57.84	57.83	57.84	57.28
323.15	66.18	66.28	66.23	66.35	66.35	64.97
			Ethyl Formate			
278.15	1.098	1.118	1.128	1.119	1.119	1.173
283.15	1.317	1.317	1.324	1.317	1.317	1.324
288.15	1.571	1.542	1.545	1.542	1.542	1.509
293.15	1.795	1.796	1.796	1.796	1.796	1.723
298.15	2.081	2.082	2.078	2.081	2.082	1.987
303.15	2.401	2.401	2.394	2.400	2.401	2.305
308.15	2.758	2.756	2.748	2.756	2.756	2.688
313.15	3.153	3.150	3.144	3.150	3.150	3.147
318.15	3.554	3.585	3.585	3.585	3.586	3.687
323.15	4.085	4.064	4.076	4.065	4.065	4.362
			Methyl Acetate			
278.15	1.829	1.836	1.856	1.815	1.814	1.896
283.15	2.075	2.096	2.108	2.084	2.084	2.106
288.15	2.377	2.382	2.386	2.379	2.379	2.349
293.15	2.691	2.696	2.691	2.700	2.701	2.630
298.15	3.033	3.038	3.027	3.049	3.049	2.953
303.15	3.430	3.410	3.395	3.424	3.424	3.324
308.15	3.850	3.813	3.797	3.827	3.826	3.750
313.15	4.306	4.248	4.238	4.257	4.257	4.237
318.15	4.626	4.718	4.718	4.716	4.715	4.797
323.15	5.235	5.222	5.243	5.202	5.202	5.433

https://doi.org/10.1021/acsomega.3c09922
ACS Omega 2024, 9, 16106−16117

Table 1. continued

T (K)	$10^3x_1^{exp}$	$10^3x_1^{van't\ Hoff}$	$10^3x_1^{\lambda h}$	$10^3x_1^{Apelblat}$	$10^3x_1^{Yaws}$	$10^3x_1^{NRTL}$
			Ethyl Acetate			
278.15	1.347	1.362	1.377	1.336	1.335	1.403
283.15	1.549	1.567	1.576	1.551	1.551	1.570
288.15	1.787	1.793	1.796	1.788	1.789	1.764
293.15	2.036	2.042	2.040	2.047	2.048	1.989
298.15	2.312	2.316	2.309	2.329	2.329	2.248
303.15	2.668	2.616	2.606	2.633	2.633	2.548
308.15	2.933	2.943	2.932	2.960	2.960	2.894
313.15	3.299	3.298	3.291	3.310	3.309	3.292
318.15	3.732	3.683	3.685	3.681	3.681	3.750
323.15	4.048	4.099	4.116	4.074	4.075	4.276
			1,4-Dioxane			
278.15	5.018	5.136	5.163	5.063	5.104	5.200
283.15	6.126	6.120	6.139	6.073	6.099	6.103
288.15	7.256	7.249	7.257	7.229	7.239	7.163
293.15	8.502	8.536	8.534	8.543	8.537	8.398
298.15	9.994	9.997	9.984	10.03	10.01	9.826
303.15	11.66	11.65	11.63	11.69	11.66	11.48
308.15	13.69	13.50	13.48	13.55	13.52	13.36
313.15	15.66	15.58	15.56	15.62	15.59	15.58
318.15	17.71	17.90	17.89	17.90	17.89	18.13
323.15	20.48	20.47	20.50	20.40	20.44	21.01

[a] x_1^{exp} is the experimental solubility of OHP in 13 pure solvents. $x_1^{van't\ Hoff}$, x_1^{Yaws}, $x_1^{Apelblat}$, $x_1^{\lambda h}$, and x_1^{NRTL} represent the calculated solubility using the van't Hoff model, Yaws model, modified Apelblat model, λh model, and NRTL model, respectively. The standard uncertainty of temperature is $u(T) = 0.05$ K and the relative standard uncertainty of pressure is $u_r(P) = 0.05$. The relative standard uncertainty of mole fraction solubility is $u_r(x_1) = 0.046$.

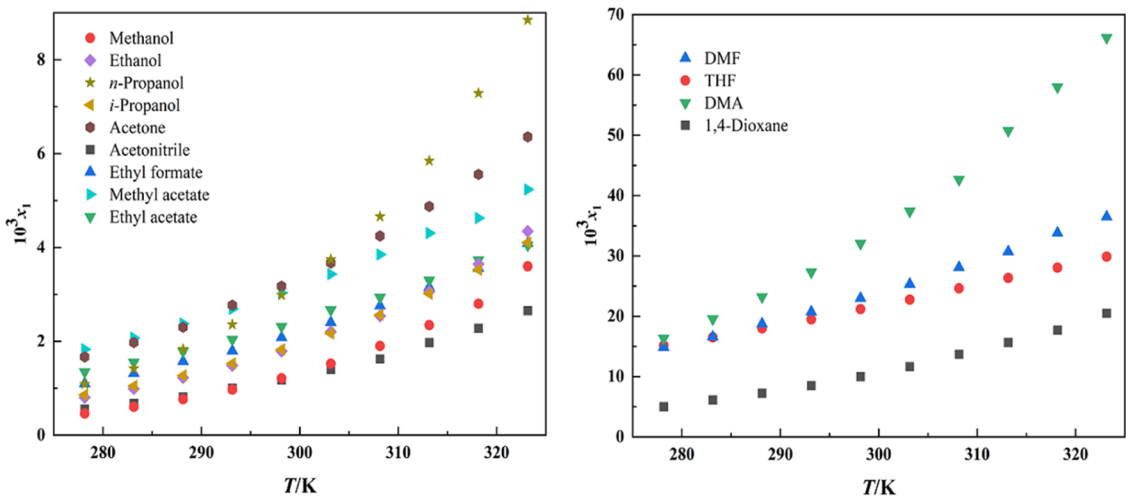

Figure 4. Mole fraction solubility of the OHP in different pure solvents.

methods used for detection, etc. Besides, the enthalpy of fusion ($\Delta_{fus}H$) of the OHP is 49.92 kJ·mol^{-1}.

2.3. Solubility Results. Table 1 summarizes the solubility data of OHP in 13 pure solvents at a temperature range of T = 278.15−323.15 K and is also clearly shown in Figure 4. As shown in Figure 4, the solubility of OHP in 13 pure solvents increased monotonically with increasing temperature monotonically. OHP is highest in DMA (0.06618 mol·mol^{-1}, 323.15 K) and the lowest in acetonitrile (0.002653 mol·mol^{-1}, 323.15 K). The difference in solubility between them is greater than 25 times. Therefore, DMA may be an ideal organic solvent considering its higher solubility and less solvent consumption. Similarly, in DMA, a higher theoretical yield can also be achieved by adjusting the temperature.

In summary, the solubility order of the OHP in 13 pure solvents is acetonitrile, methanol, ethyl formate, ethyl acetate, ethanol, *i*-propanol, acetone, *n*-propanol, 1,4-dioxane, THF, DMF, methyl acetate, and DMA. The polarity order of 13 pure solvents is 1,4-dioxane (36.0), THF (37.4), ethyl acetate (38.1), methyl acetate (38.9), ethyl formate (40.9), acetone (42.2), DMA (42.9), DMF (43.2), acetonitrile (45.6), *i*-propanol (48.4), *n*-propanol (50.7), ethanol (51.9), and methanol (55.4). The results indicate that the polarity and dipole/polarization order of the 13 solvents themselves do not match the solubility order of OHP. It follows that the solubility of OHP does not strictly follow the principle of "like dissolves like". But in different solvents, the change law of solubility is inconsistent. In alcohol solvents, the solubility order and

https://doi.org/10.1021/acsomega.3c09922
ACS Omega 2024, 9, 16106−16117

polarity value (E_T) are methanol (55.4) < ethanol (51.9) < *i*-propanol (48.4) < *n*-propanol (50.7). Except for *n*-propanol and *i*-propanol, the solubility of other solvents is negatively related to their polarity. The results show that the steric hindrances of the two solvents are different, which can explain the solubility difference of the OHP in *i*-propanol and *n*-propanol. Due to the large steric hindrance of isopropanol, it is difficult to form hydrogen bonds with OHP, which leads to the low solubility of OHP in *i*-propanol. But for ester solvents, ethyl formate (40.9) < ethyl acetate (38.1) < methyl acetate (38.9), the solubility data is positively correlated with polarity except for ethyl formate. This phenomenon can be summed up as follows: the dissolution of OHP in organic solvents is a complex process influenced by polarity and many other factors.

The results show that the change in the solubility of the OHP at different temperatures can be used as a reference for the selection of crystallization solvents. Temperature changes have a great effect on the solubility of OHP in methanol, ethanol, *n*-propanol, *i*-propanol, and acetonitrile. If the method of cooling crystallization is used, the theoretical yield can reach almost 80%. There is little change in the solubility of OHP in other organic solvents. Therefore, the solubility is an important indicator for selecting a crystallization system.

In addition, HSPs[11] had been applied for further study on the solubility order of OHP in monosolvents. From the Table 3, it can be seen that the values of δ_d of DMF, THF, DMA, *n*-propanol, acetone, and 1,4-dioxane are close to that of OHP. The δ_p values of ethanol, *i*-propanol, ethyl formate, methyl acetate, and ethyl acetate are not significantly different from those corresponding to OHP. This shows that OHP is more soluble in solvents with the same solubility parameters. This phenomenon also agrees with the "like dissolves like" principle mentioned above. In acetonitrile, the solubility of OHP is the smallest, which is related to the largest $\Delta\delta_p$ in acetonitrile. A previous literature[12] has reported that solutes exhibit poor miscibility in solvents with high δ_h values. The methanol has large δ_h values (>20), which may be the reason that the OHP shows poor solubility in this solvent. The reported literature has confirmed that, $\Delta\overline{\delta} \leq 5.0$ MPa$^{0.5}$ [13,14] and $\Delta\delta_t < 7.0$ MPa$^{0.5}$ have good mutual solubility with OHP, while the $\Delta\delta_t > 7.0$ MPa$^{0.5}$ system exhibits significantly poor mutual solubility.[15] Therefore, the OHP is more soluble in THF ($\Delta\overline{\delta} = 2.261$, $\Delta\delta_t = 2.155$) and has poor miscibility in methanol ($\Delta\delta_t = 8.005$). In summary, solvent polarity, HSPs of systems, and other factors will affect the solubility of the OHP.

2.4. Data Correlation. The van't Hoff model, λh model, the modified Apelblat model, Yaws model, and NRTL model were used to fit the solubility data of OHP in the 13 pure solvents. The calculated solubility data are also listed in Table 1. The values of the obtained model parameters relative mean deviation (RAD) and root-mean-square deviation (RMSD) are shown in Tables S1−S5. The results show that the values of RAD and RMSD are less than 1.86 and 0.0077%, respectively, in each experimental model. Therefore, it can be considered that the experimental data can be well correlated with these five models.[16] However, in the pure solvent system, the overall RAD of the Yaws model is the smallest, which shows that more accurate correlation results can be obtained using the Yaws model.

2.5. Mixing Thermodynamic Properties. In the solvent system, the thermodynamic properties of the mixture have a great influence on the solubility. The mixing Gibbs energy ($\Delta_{mix}G$), mixing enthalpy ($\Delta_{mix}H$), and mixing entropy ($\Delta_{mix}S$) can be calculated as follows

$$\Delta_{mix}G = G^E + \Delta_{mix}G^{id} \tag{1}$$

$$\Delta_{mix}H = H^E + \Delta_{mix}H^{id} \tag{2}$$

$$\Delta_{mix}S = S^E + \Delta_{mix}S^{id} \tag{3}$$

where $\Delta_{mix}G^{id}$, $\Delta_{mix}H^{id}$, $\Delta_{mix}S^{id}$ are the mixing Gibbs energy, mixing enthalpy, and mixing entropy in the ideal system, respectively, and G^E, H^E, and S^E are the excess properties.

For an ideal system, the mixing properties can be expressed by equations, as follows

$$\Delta_{mix}G^{id} = RT\sum_i^n x_i \ln x_i \tag{4}$$

$$\Delta_{mix}H^{id} = 0 \tag{5}$$

$$\Delta_{mix}S^{id} = -RT\sum_i^n x_i \ln x_i \tag{6}$$

where x_i is the mole fraction of component *i*, *R* represents the gas constant, and *T* is the solution temperature.

The excess mixing properties can be evaluated using eqs 7−9.

$$G^E = RT\sum_i^n x_i \ln \gamma_i \tag{7}$$

$$H^E = -RT^2\sum_i^n x_i\left(\frac{\partial \ln \gamma_i}{\partial T}\right)_{P,x} \tag{8}$$

$$S^E = \frac{H^E - G^E}{T} \tag{9}$$

where γ_i is the activity coefficient of component *i* in a real solution, which can be calculated by the NRTL model.

The mixing thermodynamic properties ($\Delta_{mix}G$, $\Delta_{mix}H$, $\Delta_{mix}S$) in 13 solvents were calculated and are listed in Table S6 and plotted in Figure S1. In all kinds of solvents, the values of $\Delta_{mix}G$ are negative, which shows that the OHP is spontaneously mixed in all kinds of solvents. In addition, the values of $\Delta_{mix}G$ in each solvent decrease with the increase of temperature and solubility, indicating that lower $\Delta_{mix}G$ is beneficial to dissolution.

In fact, with breaking of the regular arrangement between solvent−solvent and OHP molecules, positive entropy is more conducive to the dissolution process. But apart from in methanol and DMA, where the $\Delta_{mix}S$ value is positive, in other organic solvents, the $\Delta_{mix}S$ values are all negative. Considering that the entropy obtained by OHP in solvents other than methanol and DMA is negative, it indicates that the solute−solvent interaction will be greater in these solvents than in other interactions. This may be because the functional groups in the OHP molecules can disrupt solvent−solvent interactions through intermolecular interactions, especially hydrogen bonding with solvent molecules, resulting in the orderly arrangement of solvent molecules around solute molecules. The experimental results indicate that the dissolution process of the OHP should consider the influence of intermolecular interactions. This means that the properties of substituents on

https://doi.org/10.1021/acsomega.3c09922
ACS Omega 2024, 9, 16106−16117

the OHP molecules have a significant impact on the solute−solvent interaction.

2.6. Solvent Effect Analysis. The solid−liquid equilibrium of OHP in different solvents will be affected by many factors, such as solute and solvent properties, temperature, pressure, solvent types, and so on.[17] Table 2 lists the physicochemical properties of some experimental solvents, including polarity, summation of their hydrogen bond donor propensities, cohesive energy density, and dielectric constant.[18] In Figure S2, the solubility of the OHP is plotted according to different physicochemical properties. It is found that solvent polarity, cohesive energy density, dielectric constant, and other factors will have certain effects on the solubility of OHP in linear alcohols. The solubility of solute decreases with the increase of various properties of alcohol solvents. But its solubility in *i*-propanol is obviously not as good as that in *n*-propanol. As can be seen from Table 2, *i*-propanol has a lower hydrogen bond donor tendency than *n*-propanol. This unique dissolution phenomenon may also be related to hydroxyl groups in the molecular structure of alcohol solvents. For *i*-propanol, it is difficult for it to interact with other molecules because the hydroxyl position is different from that of *n*-propanol. Cohesive energy density is also a very important thermodynamic parameter that reflects the energy consumed per unit volume of liquid from liquid to gas. The interaction between the solute and solvent increases with the increase of cohesive energy density. In alcohol solvents, methanol has the highest cohesive energy density, which is consistent with the trend of solubility decreasing with the increase of cohesive density.

Table 2. Main Physicochemical Properties of 13 Organic Solvents[a,b,c,d],[18]

solvent	π^a	$\sum\alpha^b$	$\sum\beta^c$	cohesive energy density[d]	dielectric constant
methanol	0.6	0.43	0.47	808.26	32.61
ethanol	0.54	0.37	0.48	618.87	24.85
n-propanol	0.52	0.37	0.48	520.37	20.52
i-propanol	0.48	0.33	0.56	489.11	19.26
acetone	0.71	0.04	0.49	362.07	20.49
acetonitrile	0.75	0.07	0.32	522.95	35.69
DMF	0.88	0	0.74	463.96	37.22
THF	0.58	0	0.48	336.92	7.43
DMA	0.88	0	0.78	439.94	37.78
ethyl formate	0.61	0	0.38	339.37	8.33
methyl acetate	0.6	0	0.45	350.86	6.86
ethyl acetate	0.55	0	0.45	300.64	5.99
1,4-dioxane	0.51	0	0.64	372.17	2.21

[a]Polarity/dipolarity of the solvent. [b]Summation of the hydrogen bond donor propensities of the solvent. [c]Summation of the hydrogen bond acceptor propensities of the solvent. [d]Cohesive energy density (298.15 K) is in the unit of J·mL^3.

2.7. Apparent Thermodynamics. At the same time, this work also combined thermodynamic theory to study the specific influence of related thermodynamic functions on the dissolution process, thus deepening our understanding of the dissolution mechanism. The standard enthalpy of dissolution ($\Delta_{sol}H^\circ$), standard solution entropy ($\Delta_{sol}S^\circ$), and standard dissolution Gibbs ($\Delta_{sol}G^\circ$) of OHP were calculated according to the van't Hoff model.[19] $\Delta_{sol}H^\circ$, $\Delta_{sol}S^\circ$, and $\Delta_{sol}G^\circ$ can be expressed as follows

$$\Delta_{sol}H^\circ = -R\left(\frac{\partial \ln x}{\partial(1/T)}\right)_p = -R\left(\frac{\partial \ln x}{\partial[(1/T)-(1/T_{mean})]}\right)_p \quad (10)$$

$$\Delta_{sol}G^\circ = -RT_{mean} \times \text{intercept} \quad (11)$$

$$\Delta_{sol}S^\circ = \frac{\Delta_{sol}H^\circ - \Delta_{sol}G^\circ}{T_{mean}} \quad (12)$$

where T_{mean} represents the mean temperature (T_{mean} = 300.65 K), R is the gas constant, and "intercept" is the intercept of ln x and the $(1/T - 1/T_{mean})$ curve.

The plots of ln x versus $10^4(1/T - 1/T_{mean})$ for OHP in pure solvents at selected temperature are presented in Figure S3, which shows that it has a good linear fitting relationship with the selected solvent. In addition, the contribution rates of enthalpy and entropy of dissolution to the Gibbs energy of dissolution were estimated by using $\%\xi_H$ and $\%\xi_{TS}$. The equations for $\%\xi_H$ and $\%\xi_{TS}$ are as follows[20,21]

$$\%\xi_H = \frac{|\Delta_{sol}H^\circ|}{|\Delta_{sol}H^\circ| + |T\Delta_{sol}S^\circ|} \times 100 \quad (13)$$

$$\%\xi_{TS} = \frac{|T\Delta_{sol}S^\circ|}{|\Delta_{sol}H^\circ| + |T\Delta_{sol}S^\circ|} \times 100 \quad (14)$$

The calculated values obtained are shown in Table 3. As shown in Table 3, $\Delta_{sol}H^\circ$, $\Delta_{sol}S^\circ$, and $\Delta_{sol}G^\circ$ are all positive values in all solvents, which indicated that the dissolution process of OHP was endothermic and entropy-driven. Besides, all $\%\xi_H$ values are higher than $\%\xi_{TS}$, which showed that most of the change of molar Gibbs energy comes from entropy.

Table 3. Standard Enthalpy of Dissolution ($\Delta_{sol}H^\circ$), Standard Solution Entropy ($\Delta_{sol}S^\circ$), and Standard Dissolution Gibbs ($\Delta_{sol}G^\circ$) of OHP along with the Contribution of Dissolution Enthalpy ($\%\xi_H$) and the Contribution of Dissolution Entropy ($\%\xi_{TS}$) to the Dissolution Gibbs Energy in Different Solvents at 300.65 K

solvent	$\Delta_{sol}H^\circ$ (kJ·mol^{-1})	$\Delta_{sol}G^\circ$ (kJ·mol^{-1})	$\Delta_{sol}S^\circ$ (J·K^{-1}·mol^{-1})	ξ_H (%)	ξ_{TS} (%)
methanol	34.22	16.50	58.94	65.88	34.12
ethanol	28.09	15.57	41.64	69.17	30.83
n-propanol	34.98	14.25	68.95	62.79	37.21
i-propanol	25.98	15.55	34.72	71.34	28.66
acetone	22.19	14.19	26.60	73.51	26.49
acetonitrile	26.07	16.64	31.35	73.44	26.56
DMF	14.97	9.30	18.85	72.54	27.46
THF	11.28	9.55	5.77	86.67	13.33
DMA	23.30	8.41	49.53	61.01	38.99
ethyl formate	21.43	15.25	20.56	77.62	22.38
methyl acetate	17.36	14.34	10.02	85.21	14.79
ethyl acetate	18.29	15.01	10.90	84.80	15.20
1,4-dioxane	22.96	11.32	38.72	66.36	33.64

3. EXPERIMENTAL SECTION

3.1. Materials. OHP (white crystalline powder with a mass fraction purity of less than 0.99) was purchased from Shandong Saituo Biotechnology Co., Ltd. All 13 solvents used in the experiment were analytically pure, including methanol, ethanol, *n*-propanol, *i*-propanol, acetone, acetoni-

https://doi.org/10.1021/acsomega.3c09922
ACS Omega 2024, 9, 16106−16117

Table 4. Details Information of Materials Used[a]

chemical name	CAS no.	molar mass ($g \cdot mol^{-1}$)	source	mass fraction purity	analysis method	water content (wt %)[d]
17-α hydroxyprogesterone	68-96-2	330.46	Shandong Saituo Biotechnology Co., Ltd.	≥0.980	HPLC[b]	≤0.02%
methanol	67-56-1	32.04	Sinopharm Chemical Reagent Co., Ltd.	≥0.995	GC[c]	≤0.1%
ethanol	64-17-5	46.07	Sinopharm Chemical Reagent Co., Ltd.	≥0.997	GC[c]	≤0.3%
n-propanol	71-23-8	60.10	Sinopharm Chemical Reagent Co., Ltd.	≥0.990	GC[c]	≤0.1%
i-propanol	67-63-0	60.10	Sinopharm Chemical Reagent Co., Ltd.	≥0.997	GC[c]	≤0.1%
acetone	67-64-1	58.08	Sinopharm Chemical Reagent Co., Ltd.	≥0.995	GC[c]	≤0.3%
acetonitrile	75-05-8	41.05	Sinopharm Chemical Reagent Co., Ltd.	≥0.995	GC[c]	≤0.05%
DMF	68-12-2	73.09	Sinopharm Chemical Reagent Co., Ltd.	≥0.995	GC[c]	≤0.1%
THF	109-99-9	72.11	Sinopharm Chemical Reagent Co., Ltd.	≥0.995	GC[c]	≤0.05%
DMA	127-19-5	87.12	Sinopharm Chemical Reagent Co., Ltd.	≥0.995	GC[c]	≤0.1%
ethyl formate	109-94-4	74.08	Sinopharm Chemical Reagent Co., Ltd.	≥0.980	GC[c]	≤0.1%
methyl acetate	79-20-9	74.08	Sinopharm Chemical Reagent Co., Ltd.	≥0.980	GC[c]	≤0.1%
ethyl acetate	141-78-6	88.11	Sinopharm Chemical Reagent Co., Ltd.	≥0.995	GC[c]	≤0.1%
1,4-dioxane	123-91-1	88.11	Sinopharm Chemical Reagent Co., Ltd.	≥0.995	GC[c]	≤0.1%

[a]Both the analysis method and mass fraction purity were provided by suppliers. [b]High-performance liquid chromatography. [c]Gas chromatography. [d]The water content of OHP was determined by Karl Fischer titration. The water content of the reagent comes from the label instructions that come with the reagent.

trile, DMF, THF, DMA, ethyl formate, methyl acetate, ethyl acetate, and 1,4-dioxane. Deionized water was prepared in the laboratory (Arium Mini plus, Germany). All chemicals have not undergone any further purification; please refer to Table 4 for more detailed information.

3.2. X-ray Powder Diffraction. X-ray powder diffraction (XRPD)[22] of OHP were measured before and after the solubility experiment to confirm the uniformity of crystal form. XRPD characterization was performed on an X-ray diffractometer (Rigaku Mini Flex 600) with Cu Kα radiation. The raw materials of the OHP and 39 residual solids were determined. XRPD test conditions: a tube voltage of 40 kV, a tube current of 30 mA, and the range of diffraction angle was 3−50° (2θ) with a scan speed of $10° \cdot min^{-1}$.

3.3. Thermal Analysis. The melting point (T_m) and melting enthalpy ($\Delta_{fus}H$) of OHP were determined by differential scanning calorimetry[23] (Mettler Toledo TGA/DSC 3^+). At the heating rate of 10 $K \cdot min^{-1}$, all of the measured temperatures are between 298.15 and 623.15 K. The determination is required to be completed under nitrogen protection.

3.4. Solubility Measurements. The solubility of OHP in 13 pure solvents was measured using the static gravimetric method, with a temperature range of 278.15−323.15 K (interval 5.0 K) and a pressure of 0.1 MPa. The published literature[24] can also prove the accuracy and reliability of the static gravimetric method. The specific steps to determine the solubility are as follows: First, a certain amount of solvent, excess OHP solute, and magnetons were added into a 15 mL sample bottle. The thermostatic water-circulating bath (Ministat 230, Huber, Germany) was set to a certain temperature (with an uncertainty of ±0.05 K); then the sample bottle was added into the jacketed glass vessel filled with water, which was covered with a rubber stopper, and the magnetic stirrer was turned on for at least 12 h to ensure the solid−liquid balance. In the pre-experiment, we measured the solubility of OHP in the glass tube every hour. The results indicate that on the premise of adding excess OHP to the glass tube, the results obtained after stirring for 10 h are all equal, indicating that the solid in the glass tube is no longer dissolved and the system inside the glass tube has reached equilibrium after stirring for 10 h. To ensure the accuracy of the experimental results, we ultimately set the stirring time to 12 h. When the solid−liquid equilibrium was reached, the stirring was closed and the mixture was allowed to stand until the solid−liquid phase was completely separated. The supernatant was taken from a preheated or precooled 5 mL syringe, filtered through a 0.45 μm filter membrane, injected into an accurately weighed weighing bottle. We accurately weighed the solution and weighing bottle using an analytical balance (model AL204, Mettler Toledo, 86 Switzerland, accuracy ±0.0001g) and dried them in a vacuum drying oven at 50 °C for 48 h until the solvent had completely evaporated. Finally, we accurately weighed the quality of the dried aqueous OHP weighing bottle. All of the experimental results were measured at least three times, and the average value was taken to verify the accuracy of the data. The mole fraction solubility (x_1) of OHP in the different organic solvents was calculated based on eq 15.

$$x_1 = \frac{m_1/M_1}{m_1/M_1 + m_2/M_2} \quad (15)$$

https://doi.org/10.1021/acsomega.3c09922
ACS Omega 2024, 9, 16106−16117

Table 5. Values of Solvents Polarity, Hansen Solubility Parameters of OHP, and Selected Solvents[a,b]

solvent	polarity	δ_d (MPa$^{0.5}$)	δ_p (MPa$^{0.5}$)	δ_h (MPa$^{0.5}$)	δ_t (MPa$^{0.5}$)	$\Delta\delta_t$ (MPa$^{0.5}$)	$\Delta\bar{\delta}$ (MPa$^{0.5}$)
methanol	55.4	15.14	12.27	22.30	29.62	8.005	15.14
ethanol	51.9	15.75	8.80	19.43	26.51	4.895	11.15
n-propanol	50.7	15.95	6.80	17.39	24.56	2.945	8.765
i-propanol	48.4	15.75	6.14	16.36	23.52	1.905	7.811
acetone	42.2	15.55	10.43	6.95	19.97	1.645	6.149
acetonitrile	45.6	15.30	18.00	6.10	24.40	2.785	13.171
DMF	43.2	17.39	13.70	11.25	24.83	3.215	8.416
THF	37.4	16.80	5.70	8.00	19.46	2.155	2.261
DMA	42.9	16.80	11.50	10.20	22.77	1.155	6.241
ethyl formate	40.9	15.50	7.20	7.60	18.70	2.915	3.912
methyl acetate	38.9	15.50	7.20	7.60	18.70	2.915	3.912
ethyl acetate	38.1	15.14	5.32	9.20	18.50	3.115	3.616
1,4-dioxane	36.0	19.00	1.80	7.40	20.47	1.145	4.250
OHP		18.74	5.66	9.16	21.61		

[a]Taken from refs 15,30 and 31. [b]Reprinted (adapted or reprinted in part) with permission from 31. Copyright © 2022 American Chemical Society.

where m_1 and M_1 refer to the mass and relative molecular mass of OHP, respectively. Correspondingly, m_2 and M_2 refer to the mass and relative molecular mass of various solvents, respectively.

3.5. Solubility Data Correlation. There are currently two commonly used methods for evaluating effectiveness: one is relative mean deviation (RAD) and the other is relative root-mean-square deviation (RMSD). The thermodynamic model for calculating solubility data can be used using eqs 16 and 17[25]

$$\mathrm{RAD} = \frac{1}{n}\sum_{i}^{n}\left|\frac{x_i^{\mathrm{exp}} - x_i^{\mathrm{cal}}}{x_i^{\mathrm{exp}}}\right| \tag{16}$$

$$\mathrm{RMSD} = \left[\frac{1}{n}\sum_{i}^{n}(x_i^{\mathrm{cal}} - x_i^{\mathrm{exp}})^2\right]^{1/2} \tag{17}$$

where x_i^{exp} represents the molar fraction solubility of OHP obtained through experimental measurement and x_i^{cal} represents the molar fraction solubility of OHP calculated through the model fitting we selected. In addition, n indicates that there are several experimental temperature points.

4. THEORETICAL MODELS

In recent years, with the continuous improvement of the application value of solid−liquid equilibrium,[26,27] a large number of experienced and activity coefficient equations related to it have emerged one after another, so that many corresponding thermodynamic models have been established,[28] which can provide more theoretical basis for the determination of solubility.[29] This work selects models (containing the van't Hoff model, λh model, modified Apelblat model, Yaws model, and NRTL model) to fit the experimental solubility data.

4.1. Hansen Solubility Parameters (HSPs). The three basic Hansen solubility parameters are dispersion (δ_d), polar (δ_p), and hydrogen bonding (δ_h). The total solubility parameter (δ_{dt}) shows the total cohesive energy, defined as eq 18. On this basis, combined with experimental data, the interaction between the OHP and organic solvents can be reasonably explained.

$$\delta_t = \sqrt{\delta_d^2 + \delta_p^2 + \delta_h^2} \tag{18}$$

Values of δ_d, δ_p, and δ_h of the 13 pure solvents used in this work can be obtained directly from the literature (listed in Table 5).[15,30,31] The HSPs of OHP could be accessed by the group contribution method (listed in Table 6).[15,32]

$$\delta_d = \frac{\sum F_{d,i}}{V} \tag{19}$$

$$\delta_p = \frac{\sqrt{\sum F_{p,i}^2}}{V} \tag{20}$$

$$\delta_h = \sqrt{\frac{\sum E_{h,i}}{V}} \tag{21}$$

where the δ_d, δ_p, and δ_h are explained in detail above. The V refers to the molar volume of the OHP.

Table 6. Calculation of the Solubility Parameters (δ_d, δ_p, δ_h, δ_t) of OHP by the Group Contribution Method[a,b]

group	number	F_d ($J^{1/2}\cdot cm^{3/2}\cdot mol^{-1}$)	F_p ($J^{1/2}\cdot cm^{3/2}\cdot mol^{-1}$)	E_h ($J\cdot mol^{-1}$)
CH_3	3	420	0	0
$-CH_2-$	8	270	0	0
$=CH-$	1	320	0	0
$>C=$	1	70	0	0
$-CO-$	2	290	770	2000
$-OH$	1	210	500	20,000
ring	4	190	0	0

$\delta_d = \frac{\sum F_{d,i}}{V} = 18.7413$ MPa$^{0.5}$

$\delta_p = \frac{\sqrt{\sum F_{p,i}^2}}{V} = 5.6613$ MPa$^{0.5}$

$\delta_h = \sqrt{\frac{\sum E_{h,i}}{V}} = 9.1606$ MPa$^{0.5}$

$\delta_t = \sqrt{\delta_d^2 + \delta_p^2 + \delta_h^2} = 21.6148$ MPa$^{0.5}$

[a]Taken from refs 15 and 32. [b]Calculated by eqs 2−5.

In order to reveal the solubility of solutes in solvents, this study applied the absolute value of solute−solvent (δ_t), which is defined by the equation. Similarly, another combined solubility parameter ($\Delta\bar{\delta}$) that reveals the miscibility of two chemical substances is defined as eqs 22 and 23.

https://doi.org/10.1021/acsomega.3c09922
ACS Omega 2024, 9, 16106−16117

$$\Delta\delta_t = |\delta_{t,2} - \delta_{t,1}| \tag{22}$$

$$\Delta\overline{\delta} = [(\delta_{d2} - \delta_{d1})^2 + (\delta_{p2} - \delta_{p1})^2 + (\delta_{h2} - \delta_{h1})^2]^{0.5} \tag{23}$$

4.2. van't Hoff Model. The van't Hoff model is often used to describe the change of solubility with temperature (T/K). The model can be written as[33,34]

$$\ln x_1 = A + \frac{B}{T} \tag{24}$$

where x_1 is the mole fraction solubility of OHP and A and B are the van't Hoff parameters.

4.3. λh Model. The λh model is an empirical formula suitable for the solid−liquid equilibrium system.[35] Its expression is eq 25:

$$\ln\left[1 + \frac{\lambda(1 - x_1)}{x_1}\right] = \lambda h\left(\frac{1}{T} - \frac{1}{T_m}\right) \tag{25}$$

where λ and h are the model parameters and T_m represents the melting point of the OHP.

4.4. Modified Apelblat Model. The modified Apelblat model[36] is the most widely used semiempirical equation for correlating temperature and solubility data in pure solvent and binary mixed solvent systems.[37] It can be represented as eq 26:

$$\ln\ x_1 = A_1 + \frac{B_1}{T} + C_1 \ln T \tag{26}$$

where x_1 is the mole fraction of OHP, T is the absolute thermodynamic temperature, and A_1, B_1, and C_1 are model parameters.

4.5. Yaws Model. The Yaws model is a common empirical model used to fit solubility in pure solvents, and its expression is as follows:

$$\ln x_1 = A_2 + \frac{B_2}{T} + \frac{C_2}{T^2} \tag{27}$$

where x_1 is the mole fraction of OHP, T is the absolute thermodynamic temperature, and A_2, B_2, and C_2 are model parameters.

4.6. NRTL Model. According to the solid−liquid equilibrium theory and solute activity coefficient,[38,39] this formula provides excellent performance for many liquid solvents.[40,41] The activity coefficient can be calculated by eq 28:

$$\ln \gamma_i x_i = \frac{\Delta_{fus}H}{R}\left(\frac{1}{T_m} - \frac{1}{T}\right) \tag{28}$$

where x_1 and x_2 represent the mole fractions of solute and the selected solvents, respectively, for a pure solvent system:[42,43]

$$\ln \gamma_1 = x_2^2\left[\frac{\tau_{21}G_{21}^2}{(x_1 + x_2G_{21})^2} + \frac{\tau_{12}G_{12}^2}{(x_2 + x_2G_{12})^2}\right] \tag{29}$$

$$G_{ij} = \exp(-\alpha_{ij}\tau_{ij}) \tag{30}$$

$$\alpha_{ij} = -\alpha_{ji} = \alpha \tag{31}$$

$$\tau_{ij} = \frac{g_{ij} - g_{jj}}{RT} = \frac{\Delta g_{ij}}{RT} \tag{32}$$

where Δg_{ij} denotes the cross-interaction energy of solute and solvent molecules, R refers to the gas constant (8.314 J·mol^{-1}·K^{-1}), and α reveals the nonrandomness of the system which is an adjustable constant.

In the NRTL model, all parameters change with the temperature. Therefore, we can use α_{ij} and b_{ij} instead of parameters Δg_{ij} *and* $\Delta\lambda_{ij}$.

$$\tau_{ij} = a_{ij} + \frac{b_{ij}}{T} \tag{33}$$

5. CONCLUSIONS

This study used the gravimetric method to determine the solubility of 17-α hydroxyprogesterone (OHP) in 13 pure solvents. The solubility of the OHP in all selected solvents increases with increasing temperature. The experimental solubility data were correlated by the van't Hoff model, λh model, modified Apelblat model, Yaws model, and NRTL model. The results indicate that all models can provide satisfactory fitting results with an RAD below 5%. The HSPs were applied to study the solubility behavior. The result illustrates that the solubility sequence of the tested solvents of OHP is the result of the comprehensive effect of multiple factors. Thermodynamic properties were calculated, and the results indicated a spontaneous mixing process of the OHP in the selected solvents. Besides, $\Delta_{sol}H^\circ$, $\Delta_{sol}S^\circ$, and $\Delta_{sol}G^\circ$ proved that the dissolution process of OHP in the selected solvent is entropy-driven and endothermic. Meanwhile, the values of $\%\xi_H$ are greater than $\%\xi_{TS}$, which indicates that enthalpy plays a greater role in the standard molar Gibbs free energy.

■ ASSOCIATED CONTENT

Supporting Information

The Supporting Information is available free of charge at https://pubs.acs.org/doi/10.1021/acsomega.3c09922.

> $\Delta_{mix}G$ of OHP in different solvents, solubility of OHP in alcohol solvents at 298.15 K as a function of solvent polarity, cohesive energy density, dielectric constant, plots of ln x against $10^4(1/T - 1/T_{mean})$ for OHP in 13 pure solvents, fitting parameters of the selected models for OHP in 13 pure solvents, and thermodynamic properties of the mixing process for OHP in 13 pure organic solvents (PDF)

■ AUTHOR INFORMATION

Corresponding Author

Fumin Xue − *School of Pharmaceutical Sciences, Shandong Analysis and Test Center, Qilu University of Technology (Shandong Academy of Sciences), Jinan 250014, P. R. China*; orcid.org/0000-0002-8097-0108; Phone: 86-531-8260-5824; Email: xuefumin@qlu.edu.cn; Fax: 86-531-8296-4889

Authors

Qi Zhao − *School of Pharmaceutical Sciences, Shandong Analysis and Test Center, Qilu University of Technology (Shandong Academy of Sciences), Jinan 250014, P. R. China*

Yinhu Pan − *School of Material Science and Engineering, Shandong Jianzhu University, Jinan 250101, P. R. China*

https://doi.org/10.1021/acsomega.3c09922
ACS Omega 2024, 9, 16106−16117

Yankai Xiong − *Shandong Provincial Center for Solid Waste and Hazardous Chemical Pollution Control, Jinan 250014, P. R. China*
Ping Xu − *School of Pharmaceutical Sciences, Shandong Analysis and Test Center, Qilu University of Technology (Shandong Academy of Sciences), Jinan 250014, P. R. China*
Qianyun Sun − *Shandong Institute of Metrology, Jinan 250014, P. R. China*
Hemei Yin − *School of Pharmaceutical Sciences, Shandong Analysis and Test Center, Qilu University of Technology (Shandong Academy of Sciences), Jinan 250014, P. R. China*

Complete contact information is available at: https://pubs.acs.org/10.1021/acsomega.3c09922

Author Contributions

[⊥]Q.Z. and Y.P. contributed equally to this work and should be regarded as cofirst authors.

Notes

The authors declare no competing financial interest.

■ ACKNOWLEDGMENTS

The authors are grateful for the Shandong Provincial Natural Science Foundation (ZR2023MB036); Key R&D Program of Shandong Province, China (2021CXGC010811); Shandong Province science and technology small and medium-sized enterprises innovation ability improvement project (2022TSGC1011); Jinan Introducing Innovation Team Project (202228033); and the Talent Research Project of Qilu University of Technology (2023RCKY076).

■ REFERENCES

(1) Karaguzel, G.; Eyuboglu, I.; Ozdem, S.; Kader, S.; Kaya, S.; Beyhun, N. E. Reference intervals for serum 17alpha-hydroxyprogesterone and ultrasonographic adrenal gland sizes in healthy newborns. *J. Matern.-Fetal Neonat. Med.* **2020**, *33*, 3998−4003.
(2) Morejón García, G.; García de la Rosa, I.; González Reyes, E. C.; Rubio Torres, A.; Quintana Guerra, J. M.; Hernández Marín, M.; Pérez Mora, P. L.; Feal Carballo, S.; Lafita Delfino, Y.; Pupo Infante, M.; Castells Martínez, E. M.; Rosabal Poloshkov, A.; Hernández Pérez, L. Generation of monoclonal antibodies against 17α-hydroxyprogesterone for newborn screening of congenital adrenal hyperplasia. *Clin. Chim. Acta* **2018**, *485*, 311−315.
(3) Liu, J.; Pang, Z.; Wang, G.; Guan, X.; Fang, K.; Wang, Z.; Wang, F. Advanced role of neutrophils in common respiratory diseases. *J. Immunol Res.* **2017**, *2017*, No. 6710278.
(4) Cañas, J. A.; Sastre, B.; Mazzeo, C.; Fernández-Nieto, M.; Rodrigo-Muñoz, J. M.; González-Guerra, A.; Izquierdo, M.; Barranco, P.; Quirce, S.; Sastre, J.; del Pozo, V. Exosomes from eosinophils autoregulate and promote eosinophil functions. *J. Leukocyte Biol.* **2017**, *101*, 1191−1199.
(5) Pérez-Ciria, L.; Miana-Mena, F. J.; Falceto, M. V.; Mitjana, O.; Latorre, M. A. Effect of immunocastration and diet on growth performance, serum metabolites and sex hormones, reproductive organ development and carcass quality of heavy gilts. *Animals* **2021**, *11*, No. 1900, DOI: 10.3390/ani11071900.
(6) Bullen, J. A. Studies of medical tests: Design and analytical considerations. *Chest* **2020**, *158*, S103−S112.
(7) American College of Clinical Pharmacy. Standards of practice for clinical pharmacists. *Pharmacotherapy* **2014**, *34*, 794−797, DOI: 10.1002/phar.1438.
(8) Nelson, D. B.; McIntire, D. D.; Leveno, K. J. A chronicle of the 17-alpha hydroxyprogesterone caproate story to prevent recurrent preterm birth. *Am. J. Obstet. Gynecol.* **2021**, *224*, 175−186.
(9) Manzurola, E.; Apelblat, A. Solubilities of l-glutamic acid, 3-nitrobenzoic acid, p-toluic acid, calcium-l-lactate, calcium gluconate, magnesium-dl-aspartate, and magnesium-l-lactate in water. *J. Chem. Thermodyn.* **2002**, *34*, 1127−1136.
(10) Tikkanen, I.; Narko, K.; Zeller, C.; Green, A.; Salsali, A.; Broedl, U. C.; Woerle, H. J. Empagliflozin reduces blood pressure in patients with type 2 diabetes and hypertension. *Diabetes Care* **2015**, *38*, 420−428.
(11) Jafari, P.; Barzegar-Jalali, M.; Jouyban, A. Solubility of mesalazine in aqueous solutions of two betaine-based deep eutectic solvents at different temperatures: Data correlation and thermodynamic analysis. *J. Mol. Liq.* **2022**, *366*, No. 120306, DOI: 10.1016/j.molliq.2022.120306.
(12) Takebayashi, Y.; Morii, N.; Sue, K.; Furuya, T.; Yoda, S.; Ikemizu, D.; Taka, H. Solubility of n,n′-di(1-naphthyl)-n,n′-diphenyl benzidine (npb) in various organic solvents: Measurement and correlation with the hansen solubility parameter. *Ind. Eng. Chem. Res.* **2015**, *54*, 8801−8808.
(13) Güner, A. The algorithmic calculations of solubility parameter for the determination of interactions in dextran/certain polar solvent systems. *Eur. Polym. J.* **2004**, *40*, 1587−1594.
(14) Alanazi, A.; Alshehri, S.; Altamimi, M.; Shakeel, F. Solubility determination and three dimensional hansen solubility parameters of gefitinib in different organic solvents: Experimental and computational approaches. *J. Mol. Liq.* **2020**, *299*, No. 112211.
(15) Mohammad, M. A.; Alhalaweh, A.; Velaga, S. P. Hansen solubility parameter as a tool to predict cocrystal formation. *Int. J. Pharm.* **2011**, *407*, 63−71.
(16) Huang, W.; Wang, H.; Li, C.; Wen, T.; Xu, J.; Ouyang, J.; Zhang, C. Measurement and correlation of solubility, hansen solubility parameters and thermodynamic behavior of clozapine in eleven mono-solvents. *J. Mol. Liq.* **2021**, *333*, No. 115894.
(17) Wang, Y.; Cai, L.; Du, S.; Cheng, Y.; Zhang, P.; Li, Y.; Xue, F.; Gong, J. Solid-liquid equilibrium of ropivacaine in fourteen organic solvents: An experimental and molecular simulation study. *J. Mol. Liq.* **2022**, *349*, No. 118163.
(18) Gu, C.-H.; Li, H.; Gandhi, R. B.; Raghavan, K. Grouping solvents by statistical analysis of solvent property parameters: Implication to polymorph screening. *Int. J. Pharm.* **2004**, *283*, 117−125.
(19) Li, M.; Gao, Z.; Li, Z.; Wang, Z.; Zhou, R.; Wang, B. Determination and correlation of solubility of 4,4′-difluorobenzophenone in pure and binary mixed solvents and thermodynamic properties of solution. *J. Mol. Liq.* **2020**, *317*, No. 113903.
(20) Visscher, F.; Gaakeer, W. A.; Granados Mendoza, P.; de Croon, M. H. J. M.; van der Schaaf, J.; Schouten, J. C. Liquid−liquid extraction systems of benzoic acid in water and heptane, methylbenzene, or trichloroethylene as cosolvent. *J. Chem. Eng. Data* **2011**, *56*, 3630−3636.
(21) Yang, Z.-H.; Zeng, Z.-X.; Sun, L.; Xue, W.-L.; Chen, N. Determination and correlation of solubilities of lauric acid in eight alcohols. *J. Chem. Eng. Data* **2014**, *59*, 2725−2731.
(22) Wang, Q.; Bian, X.; Chen, X. X-ray powder diffraction data for 17-hydroxy-16-methyl-9,11-epoxypregna-1,4,6-triene-3,20-dione, c22h26o4. *Powder Diffr.* **2019**, *34*, 279−281.
(23) Leyva-Porras, C.; Cruz-Alcantar, P.; Espinosa-Solis, V.; Martinez-Guerra, E.; Balderrama, C. I. P.; Martinez, I. C.; Saavedra-Leos, M. Z. Application of differential scanning calorimetry (dsc) and modulated differential scanning calorimetry (mdsc) in food and drug industries. *Polymers* **2020**, *12*, No. 5, DOI: 10.3390/polym12010005.
(24) Granberg, R. A.; Rasmuson, Å. C. Solubility of paracetamol in pure solvents. *J. Chem. Eng. Data* **1999**, *44*, 1391−1395.
(25) Yang, L.; Yin, Q.; Hou, B.; Wang, Y.; Bao, Y.; Wang, J.; Hao, H. Solubility and thermodynamic stability of the enantiotropic polymorphs of 2,3,5-trimethyl-1,4-diacetoxybenzene. *Ind. Eng. Chem. Res.* **2013**, *52*, 2477−2485.
(26) Shi, Y.; Yu, G.; Wang, X. Experimental determination and thermodynamic modeling of solid-liquid equilibrium of 2,6-dimethylphenol, 3,5-dimethylphenol and 2,5-dimethylphenol binary and ternary systems. *Thermochim. Acta* **2022**, *710*, No. 179174.

(27) Ma, Y.; Wu, S.; Macaringue, E. G. J.; Zhang, T.; Gong, J.; Wang, J. Recent progress in continuous crystallization of pharmaceutical products: Precise preparation and control. *Org. Process Res. Dev.* **2020**, *24*, 1785−1801.
(28) Winter, B.; Winter, C.; Esper, T.; Schilling, J.; Bardow, A. Spt-nrtl: A physics-guided machine learning model to predict thermodynamically consistent activity coefficients. *Fluid Phase Equilib.* **2023**, *568*, No. 113731.
(29) Li, Y.; Alameri, A. A.; Farhan, Z. A.; Ai_Sadi, H. l.; Alosaimi, M. E.; Ghaleb AbdalSalam, A.; Jumaah Jasim, D.; Hadrawi, S. K.; Mohammed Al-Taee, M.; Lafta, A. H.; Othman, H. A.; Mousa Alzahrani, S.; Moniem, A. A.; Alqadi, T. Theoretical modeling study on preparation of nanosized drugs using supercritical-based processing: Determination of solubility of chlorothiazide in supercritical carbon dioxide. *J. Mol. Liq.* **2023**, *370*, No. 120984.
(30) Ouyang, J.; Liu, L.; Zhou, L.; Liu, Z.; Li, Y.; Zhang, C. Solubility, dissolution thermodynamics, hansen solubility parameter and molecular simulation of 4-chlorobenzophenone with different solvents. *J. Mol. Liq.* **2022**, *360*, No. 119438.
(31) Shen, Y.; Li, R.; Zhao, P.; Liu, W.; Yang, X.; Zhang, Z. Equilibrium solubility of 18β-glycyrrhetinic acid in 12 pure solvents: Determination, correlation, and hansen solubility parameter. *J. Chem. Eng. Data* **2022**, *67*, 3243−3251.
(32) Sun, R.; He, H.; Wan, Y.; Li, L.; Sha, J.; Jiang, G.; Li, Y.; Li, T.; Ren, B. Kojic acid in fourteen mono-solvents: Solubility data, hansen solubility parameter and thermodynamic properties. *J. Chem. Thermodyn.* **2021**, *152*, No. 106280.
(33) Grant, D. J. W.; Mehdizadeh, M.; Chow, A. H. L.; Fairbrother, J. E. Non-linear van't hoff solubility-temperature plots and their pharmaceutical interpretation. *Int. J. Pharm.* **1984**, *18*, 25−38.
(34) Deiters, U. K. The isothermal van't hoff equation for phase equilibria—a forgotten relation? *Fluid Phase Equilib.* **2012**, *336*, 22−27.
(35) Wang, Z.; Yu, S.; Li, H.; Liu, B.; Xia, Y.; Guo, J.; Xue, F. Solid−liquid equilibrium behavior and solvent effect of gliclazide in mono- and binary solvents. *ACS Omega* **2022**, *7*, 37663−37673.
(36) Share Mohammadi, H.; Asl, A. H.; Khajenoori, M. Determination of amiodarone hydrochloride solubility in pure and ethanol-modified subcritical water: Experimental data and modeling. *J. Mol. Liq.* **2022**, *362*, No. 119679, DOI: 10.1016/j.molliq.2022.119679.
(37) Yu, C.; Sun, X.; Wang, Y.; Du, S.; Shu, L.; Sun, Q.; Xue, F. Determination and correlation of solubility of metformin hydrochloride in aqueous binary solvents from 283.15 to 323.15 k. *ACS Omega* **2022**, *7*, 8591−8600.
(38) Chen, J.; Xu, R.; Zhu, P.; Zhao, H. Solubility and mixing thermodynamic properties of triclabendazole in 14 neat solvents at elevated temperatures from 278.15 to 318.15 k. *J. Chem. Eng. Data* **2021**, *66*, 3598−3607.
(39) Hong, W.; Jia, S.; Li, Z.; Li, W.; Gao, Z. Solubility determination and thermodynamic correlation of chlorphenesin in 12 pure solvents from 288.15 to 328.15 k. *J. Chem. Eng. Data* **2021**, *66*, 822−831.
(40) Wang, G.; Wang, G.; Gong, J.; Li, W.; Shang, Z.; Zhao, S.; Dong, W.; Wang, Y. Experimental determination and computational analysis of solid−liquid phase equilibrium of nifedipine in twelve pure solvents. *J. Chem. Thermodyn.* **2020**, *150*, No. 106223.
(41) Fang, Z.; Zhang, L.; Mao, S.; Rohani, S.; Ulrich, J.; Lu, J. Solubility measurement and prediction of clopidogrel hydrogen sulfate polymorphs in isopropanol and ethyl acetate. *J. Chem. Thermodyn.* **2015**, *90*, 71−78.
(42) Chen, F.-x.; Qi, Z.-l.; Feng, L.; Miao, J.-y.; Ren, B.-Z. Application of the nrtl method to correlate solubility of diosgenin. *J. Chem. Thermodyn.* **2014**, *71*, 231−235.
(43) Li, J.; Hao, H.; Guo, N.; Wang, N.; Hao, Y.; Luan, Y.; Chen, K.; Huang, X. Solubility and thermodynamic properties of maltol in different pure solvents. *J. Mol. Liq.* **2017**, *243*, 313−323.

https://doi.org/10.1021/acsomega.3c09922
ACS Omega 2024, 9, 16106−16117